ACS APPLIED MATERIALS & INTERFACES

RESEARCH ARTICLE

www.acsami.org

Silica Shell/Gold Core Nanoparticles: Correlating Shell Thickness with the Plasmonic Red Shift upon Aggregation

Alan Vanderkooy, Yang Chen, Ferdinand Gonzaga, and Michael A. Brook*

Department of Chemistry and Chemical Biology, McMaster University, 1280 Main Street West, Hamilton, Ontario, Canada L8S 4M1

Supporting Information

ABSTRACT: Differences in the wavelengths of the surface plasmon band of gold nanoparticles (AuNP) — before and after particle aggregation — are widely used in bioanalytical assays. However, the gold surfaces in such bioassays can suffer from exchange and desorption of noncovalently bound ligands and from nonspecific adsorption of biomolecules. Silica shells on the surfaces of the gold can extend the available surface chemistries for bioconjugation and potentially avoid these issues. Therefore, silica was grown on gold surfaces using either hydrolysis/condensation of tetraethyl orthosilicate **1** under basic conditions or diglyceroxysilane **2** at neutral pH. The former precursor permitted slow, controlled growth of shells from about 1.7 to 4.3 nm thickness. By contrast, 3−4 nm thick silica shells formed within an hour using diglyceroxysilane; thinner or thicker shells were not readily available. Within the range of shell thicknesses synthesized, the presence of a silica shell on the gold nanoparticle did not significantly affect the absorbance maximum (∼ 5 nm) of unaggregated particles. However, the change in absorbance wavelength upon aggregation of the particles was highly dependent on the thickness of the shell. With silica shells coating the AuNP, there was a significant decrease in the absorbance maximum of the aggregated particles, from ∼578 to ∼536 nm, as the shell thicknesses increased from ∼1.7 to ∼4.3 nm, because of increased distance between adjacent gold cores. These studies provide guidance for the development of colorimetric assays using silica-coated AuNP.

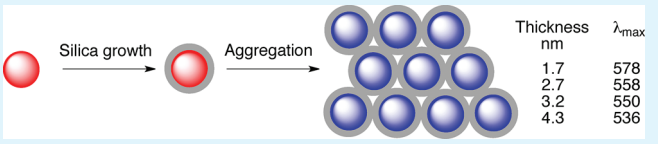

KEYWORDS: gold nanoparticle, silica shell, plasmon, aggregation, assay, interparticle, core−shell, red shift, diglycerylsilane

INTRODUCTION

Noble metal nanoparticles exhibit physical properties distinct from analogous atomic or bulk materials. Gold nanoparticles (AuNP), in particular, have undergone a recent renaissance because of their unusual photoproperties, which have been adapted for a variety of biological and analytical colorimetric assays that exploit the surface plasmon band (SPB).[1] The SPB is size dependent and is red-shifted with increasing particle size.[2] The absorption spectrum of gold nanoparticles (AuNP) of 13 nm diameter, for example, shows maximum absorbance at 520 nm such that colloidal dispersions exhibit a burgundy-red color.[3]

A key property of AuNP is that the plasmon can also be red-shifted by aggregating the particles (Figure 1A). That is, if small particles are brought into close proximity through van der Waals forces, for instance, by screening or neutralizing stabilizing charges on the surface of the particles (e.g., by increasing the solution ionic strength), the absorbance maximum red shifts and the visible appearance of the particles shifts from red to purple or blue. The color changes that accompany nanoparticle aggregation, when initiated by biological events, are particularly useful in biological assays.

In a practical sense, to be used in an assay, the color change that accompanies aggregation needs to be sufficiently profound such that on/off (positive/negative) decisions about the presence of the analytes can be determined with the naked eye. Aggregation is not an "all or nothing" phenomenon: a continuum of colors can be observed for AuNP aggregated, for example, at different ionic strengths. The AuNP absorbance shift increases both with increasing aggregate size and with decreasing interparticle distance.[1,4−6] Aggregates, which are more strongly stabilized in a colloidal sense than isolated particles, are "self-stabilizing",[7,8] and give rise to a "primary minimum" aggregate size under a given set of conditions. To be useful, aggregates should have a readily distinguishable color from the unaggregated AuNP, within a reasonable time. It should be possible to exhibit some control over aggregation by constraining the interparticle distance between AuNP within aggregates by using a silica shell.

The particle size-dependent photophenomenon associated with the SPB was first described mathematically by Mie via solution of the Maxwell equations.[9] The observed absorption spectrum results from the oscillation of the electron cloud (plasmon) within the metal nanoparticle. The frequency of the plasmon is constrained by the radius of the nanoparticle and thus only light of similar wavelength as the resonance frequency will be absorbed/scattered. As the particles come into close proximity, the plasmons couple together and the resonance frequency red shifts. For a review, the reader is referred to Ghosh and Pal.[6]

Several studies have described, both theoretically and experimentally, the dependence of the plasmon on interparticle distance for idealized systems such as dimers or thin films.[10−20]

Received: June 26, 2011
Accepted: September 1, 2011
Published: September 01, 2011

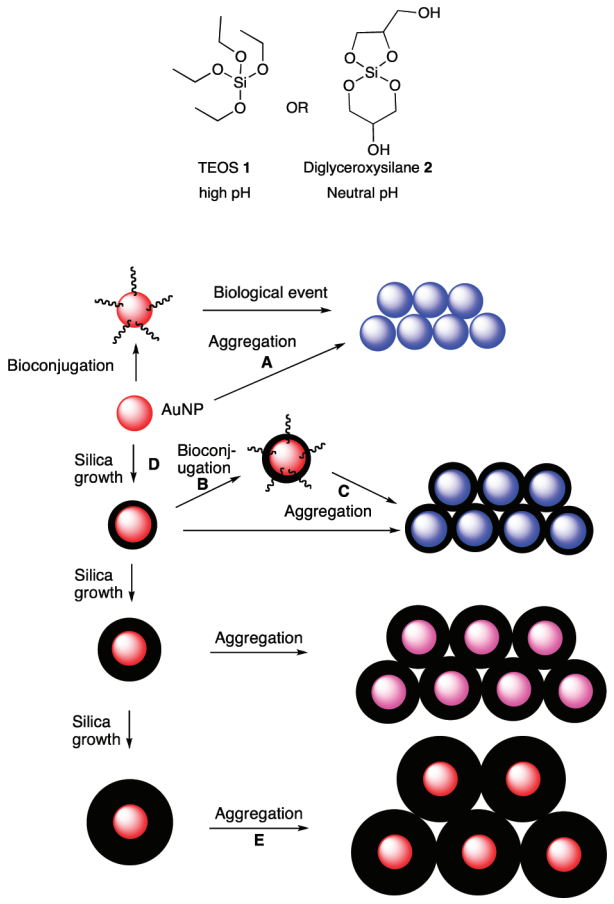

Figure 1. Top: Silane precursors used for silica shell growth. Bottom: Packing of AuNP with different shell thicknesses. Upon aggregation, changes in maximum wavelength of absorption are larger with thinner silica shells.

Of particular relevance to the present study is an examination of UV activity of layers of silica coated AuNP, in which interparticle distance in thin films was constrained by silica shell thickness.[11] There exist few studies that examine the effect of interparticle distance on the plasmon of aggregates in solution.

In nanoscience, silica is often used to define the space between other nanostructures, and it further finds utility because of biocompatibility, transparency, and the ability to provide a convenient chemical anchor for (bio)conjugation.[21−24] Silica displays low nonspecific adsorption of biomolecules and as such is an attractive surface coating for AuNP to be used in biosensors.

Gold surfaces can suffer from exchange and desorption of noncovalently bound ligands[25] and from nonspecific adsorption of biomolecules.[26] Liu and co-workers have previously described biofunctionalization and aggregation-based assays using silica encapsulated AuNP (SiO_2−AuNP).[27−29] However, because of the thickness of shells used, the particles do not display a color change upon aggregation, which diminishes the practical utility of the assay.

Improved bioassays using AuNP would result from robust silica surface layers on the gold, to which biological entities could be reliably tethered (Figure 1B), and which would undergo obvious color changes − due to particle aggregation − in response to a biological event (Figure 1C). The latter requires a synthetic route that will cover the gold with silica completely, but at a thickness at which the plasmon changes upon aggregation are obvious (Figure 1B,C vs E).

In the current study, SiO_2−AuNP were synthesized with varying shell thicknesses in order to constrain the interparticle distance upon aggregation. These studies permit a correlation of interparticle distance with plasmonic red shift, which is important in developing SiO_2−AuNP−based colorimetric assays. The polyvinylpyrrolidone (PVP) method[30] was used to prime AuNP followed by subsequent Stöber silica growth[31] with varying incubation times and concentrations of tetraethyl orthosilicate (**1**, TEOS) to control shell thickness. The use of TEOS for synthesis of SiO_2−AuNP, was compared with diglyceroxysilane **2**, a silica precursor that can be used in water at neutral pH (Figure 1). The model particles were aggregated using salt (rather than by biologically driven events). To the best of our knowledge, this study presents the first description of plasmonic red shifts of SiO_2−AuNP upon aggregation that occur in solution, by manipulating the interparticle distance through an ultrathin (less than about 4.3 nm) silica shell. The use of such a thin silica shell on AuNPs allows aggregation to be visually observed (using the naked eye) in a convenient time-scale for a colorimetric assay, and furthermore, provides alternate chemistry for subsequent surface modification.

EXPERIMENTAL SECTION

Materials. Tetrachloroauric acid trihydrate, polyvinylpyrrolidone (PVP, MW ∼10 000), tetraethyl orthosilicate (TEOS) (99.999%) and tetramethyl orthosilicate (TMOS) (98%) were purchased from Sigma-Aldrich. Trisodium citrate dihydrate was purchased from EM Science. Magnesium chloride hexahydrate and 28−30% ammonium hydroxide were purchased from EMD Chemicals. Anhydrous glycerol was purchased from Fluka.

Characterization. UV−vis spectroscopy was performed using a Cary 50 Probe UV−vis Spectrophotometer and a Tecan Infinite M200 plate reader. Transmission electron microscopy was performed using a JEOL JEM-1200EX TEMSCAN. Particle sizes and thickness of silica shells on AuNP were determined using Image J software.

Synthesis of Citrate−AuNP. The synthesis of spherical citrate−AuNP of 13.5 nm was based on a previously described procedure.[32] Briefly, 200 mL of 0.24 mM aqueous tetrachloroauric acid trihydrate was heated to 80 °C. To this was added trisodium citrate dihydrate (0.94 mL of an aqueous 0.34 M solution). This mixture was heated at 80 °C overnight and subsequently allowed to cool to room temperature. The particles were used as prepared and characterized by UV−vis spectroscopy and transmission electron microscopy. Using the extinction coefficient given by Maye et al.,[33] the concentration of AuNP was determined to be 4.2 nM.

TEOS Mediated Synthesis of SiO_2−AuNP. Silica was grown on AuNP using TEOS-mediated synthesis based on a previously described Stöber-like method.[30] PVP (MW ∼10 000, 0.840 mL of 25.6 g/L, 2.15 mmol) was added to Cit−AuNP (45 mL, 4.2 nM). After stirring for 24 h, the mixture was split into two and each portion was centrifuged at 14 000 g for 50 min and recombined in 26 mL of ethanol (PVP−AuNP in EtOH). To PVP−AuNP in EtOH solution (18 mL) was added TEOS (180 μL, 0.81 mM, 1% v/v) followed by ammonia (0.9 mL of 0.62 M in 95.8% ethanol, 0.56 mmol).

The effect of incubation time was explored by interrupting shell growth at time points 6.6, 15.6, 25, and 40 h by adding 4 mL of the particle growth solution to 16 mL of H_2O, centrifuging for 45 min and resuspending three times in H_2O. The first two resuspensions were made up to 20 mL H_2O. The third and final resuspension was made up to 7.5 mL of H_2O.

The effect of different concentrations of TEOS on the rate of shell growth were examined by adding either 120 or 20 μL TEOS

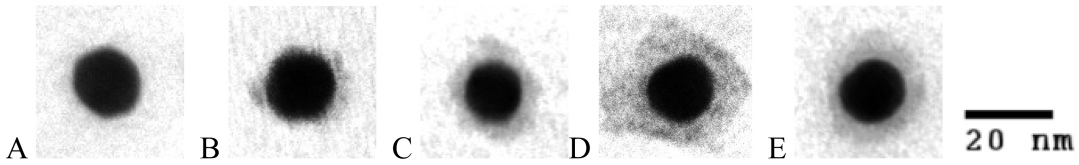

Figure 2. (A) Unmodified AuNP. (B) Thin shell after 6.6 h of Stöber growth at 1% TEOS v/v showing islands. (C) Shells after 15.6 h of Stöber growth at 1% TEOS v/v. (D) Shells after 40 h of Stöber growth at 1% TEOS v/v. (E) Diglyceroxysilane **2** derived silica shells after 45 min of growth at 1% **2** w/w.

(3% and 0.5% v/v) to 4 mL of PVP-AuNP in EtOH, followed by the addition of NH_4OH (0.2 mL of 0.62 M in 95.8% ethanol, 0.12 mmol). The resulting particles were incubated for 40 h and worked up in the same manner as above (centrifugation and washing). The thickness of the shells was examined using transmission electron microscopy and size determined using the measure function of Image J software.[34]

Diglyceroxysilane-Mediated Synthesis of SiO_2—AuNP. The surface modification of gold with diglyceroxysilane (**2**) as the silica precursor required a different procedure. Compound **2** was prepared from TMOS and glycerol according to a previously described procedure involving the transesterification of TMOS with glycerol.[35] Compound **2** was ground to a fine powder with a mortar and pestle and then dissolved in H_2O by sonicating in an ice bath for 20 min. The sample was filtered through a 0.45 μm cellulose acetate filter to remove any undissolved material. PVP—AuNP in H_2O (52 mL) were generated as described above, except that they were resuspended in H_2O rather than EtOH. To PVP—AuNP in H_2O (18 mL) was added fresh, aqueous **2** (1.8 mL, 10% w/v, 0.82 mM). The effect of incubation time was explored by interrupting shell growth at time points 0.75, 1.8, 2.8, 3.9, 6.6, 15.6, 25, and 40 h, by the same method as used for the TEOS-derived particles.

The effect of different concentrations of **2** was examined by adding 0.4 mL of either 30% or 5% w/v aqueous **2** solution to 4 mL of PVP—AuNP suspended in H_2O. These were incubated for 40 h and worked up in the same manner as above. The thickness of the shells was examined with transmission electron microscopy and measured using Image J software.

Correlating Shell Thickness to Plasmon Shift. To examine the effect of shell thickness on the plasmon shift associated with aggregation, 1 mL of different particle samples were mixed with 1 g of $MgCl_2 \cdot 6H_2O$ and transferred to the well of a 48 well plate. The absorption spectra were taken at times 2 h, 1 day, and 4 days after mixing.

RESULTS

Silica Shell Synthesis. SiO_2—AuNP core—shell particles were first synthesized by Liz-Marzán et al.[36,37] They primed citrate-coated AuNP (Cit—AuNP) with aminopropyltrimethoxysilane and then grew a silica shell using sodium silicate at pH 8.5 in water. Larger shells could then be synthesized by transfer into ethanol followed by a Stöber growth process.[36,38] Other researchers have prepared SiO_2—AuNP by using polyvinyl-pyrrolidone (PVP) to prime AuNP and avoid the initial sodium silicate shell growth;[30] different silanes to prime AuNP;[39−41] Stöber growth directly on Cit-AuNP, thus eliminating the priming step;[32,42] ammonium-catalyzed hydrolysis and condensation of TEOS on hydrophobic particles via a cationic micelles;[43] and reverse microemulsion-mediated synthesis.[44] For a review on the topic, the reader is referred to Liu and Han.[23] We chose to use the PVP primed route.[30]

Silica shells were grown on AuNP (Figure 2A) using two distinct protocols: sol—gel condensation of TEOS at high pH in ethanol and with **2**[35] at neutral pH in water. It was possible to synthesize relatively thin silica shells, compared to shells

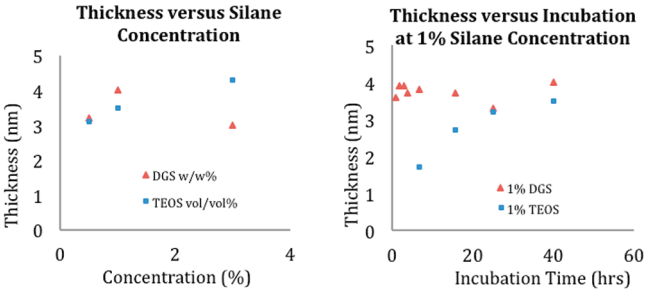

Figure 3. Thickness of shells as a function of (A) alkoxysilane concentration, and (B) incubation time. DGS = **2**.

described in the literature, without switching solvents by utilizing **2**. Compound **2** also led to formation of silica shells very quickly: treatment of 13.5 nm PVP-AuNP with **2** in H_2O led to the formation of well-defined, nearly spherical shells within 45 min (Figure 2E). The use of different concentrations of **2** and incubation times were examined to establish if it is possible to control the shell thickness. Attempts to make either thinner or thicker shells by varying the synthesis protocol have been unsuccessful: the thickness of the deposited silica shell consistently ranged between 3 and 4 nm. There is thus no apparent correlation between shell thickness and incubation time or between shell thickness and concentration of **2** (Figure 3).

The formation of silica on gold when using **1** at high pH — the Stöber method[31] — occurred more slowly than the reaction with **2**. In the former case, silica begins to be deposited on AuNP after ~6.6 h (Figure 2B). However, at that time point TEM showed small silica islands deposited on a bare gold surface. Complete encapsulation was first observed at 15.6 h (Figure 2C). Unlike the process with **2**, the use of TEOS at high pH showed a positive correlation between silica shell thickness and both incubation time and TEOS concentration. Shell thicknesses ranged from 1.7 to 4.3 nm.

The Stöber-based TEOS (**1**) and diglyceroxysilane (**2**) methods led to silica shells of similar, nearly spherical shape. In both cases, secondary nucleated (pure silica) particles were observed at longer incubation times and at higher silane precursor concentrations.

AuNP Absorption Maxima. Prior to surface modification, the Cit-AuNP were red in color with maximum absorbance at 521 nm. There were relatively minor differences in the wavelengths of maximum absorbance of the unaggregated AuNP after growth of the silica shell irrespective of thickness. The absorbance maxima on the SiO_2—AuNP only changed subtly from the precursor particle, from 521 nm to between 525 and 527 nm, with the exception of Stöber growth shells that were stopped at 6.6 h (new absorbance maximum, 543 nm), in which case silica shells did not completely encapsulate the AuNP.

AuNP Absorption Maxima after Aggregation. Ultimately, SiO_2—AuNP are designed to be used in bioassays in which

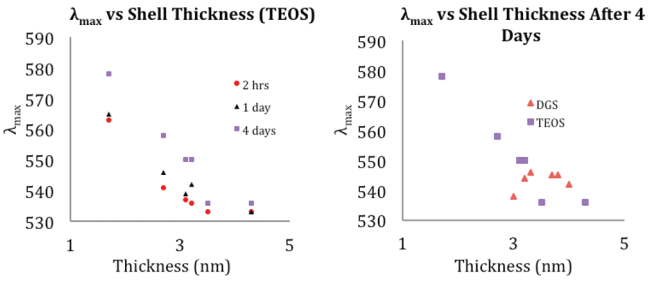

Figure 4. Comparison of red shifts with silica shell thickness over time. A) Stöber growth particles after different aggregation times. (B) Comparison of red shift of **2**-synthesized particles and those grown with the Stöber-like method after 4 days of aggregation. DGS = **2**.

aggregation leads to profound, readily detected color changes following a biological event. Here, however, the particles were aggregated using high $MgCl_2$ concentrations as part of model studies. The maximum absorbances were observed to red shift over time, presumably because of increasing aggregate size: compare, for example, the absorbance maximum of the nanoparticles with a 2.7 nm silica shell that changes from 541 to 546 to 558 nm at 1, 2, and 4 days, respectively. AuNP with thinner silica shells showed greater red shifts: a negative correlation can be seen between λ_{max} and shell thickness (Figure 4) for TEOS derived core−shell particles. Core−shell particles derived from **2** did not have a large enough range of silica thicknesses to establish a trend in λ_{max} upon aggregation, however, the observed SPB upon particle aggregation fit well with the trend established by TEOS-derived core−shell particles.

DISCUSSION

Silica Growth. The evolution of silica, formed in a sol−gel process from alkoxysilanes, is well-understood. At high pH, as in the Stöber process,[31] alkoxysilanes undergo efficient hydrolysis and less effective condensation. The primary particles that first appear after oligomerization are electrostatically stabilized by silanolate (R_3SiO^-) groups on the surface. When properly controlled, particles that subsequently form are captured by the primary particles, leading to a steady increase in the average diameter of relatively monodisperse particles.

A very similar growth process was observed with the PVP-modified AuNP when TEOS was used as the silica precursor at high pH. The PVP coating[30] serves as a surface to which silica particles show affinity[45] and, once a silica shell is formed, on which the silica shells thicken. The large size of the gold particle assures, at least in the early stages of the process, that secondary nucleation of silica particles is a relatively inefficient process. Initially, formation of a shell did not occur homogeneously across the surface: islands of silica formed (Figure 2B). Because few secondarily nucleated silica particles were observed in the early stage of silica formation, we ascribe islanding to facilitated growth in the region of adsorbed silica. Eventually the "bare spots" filled in and the thickness of the silica shell on these surfaces followed a very smooth increase as a function of TEOS concentration (Figure 3A), and as a function of time (Figure 3B).

The conversion of **2** to silica was previously shown to follow a very different mechanistic process. First, unlike TEOS, the starting material is soluble in water at neutral pH, and there is no induction time for the conversion of two phases into one, as occurs with TEOS or TMOS.[35,46,47] Second, unlike the rates for alkoxysilane hydrolysis, which are usually accelerated at pHs away from neutrality,[22] **2** rapidly hydrolyzes at pH 7,[35] a pH at which silanols also undergo efficient condensation to disiloxanes.[48]

When **2** was hydrolyzed at neutral pH in the presence of gold nanoparticles, silica shells rapidly formed on the PVP primed gold surface. However, unlike the case with TEOS, it was difficult to control the thickness of the shell by manipulating the concentration of **2** or the length of incubation: irrespective of these conditions, ∼4 nm thick silica shells rapidly formed and then ceased to grow (Figure 3). Because shells grew faster from **2** than from **1**, it was possible to obtain cleaner particles with essentially no secondary nucleation.

This unusual behavior may be attributed to the chemistry of **2** when compared to TEOS and also to the nature of colloidal stabilization at neutral pH in the case of **2**. The kinetics of condensation of **2** are not very sensitive to pH, but are very sensitive to ionic strength.[49] The charge at the gold surface, arising from citrate and PVP,[50] will accelerate silica formation from **2** at the gold interface until the charge is screened by the newly formed silica layer. At neutral pH, the lower surface charge on the formed silica will be associated with lower electrostatic stabilization. The gold particles capture the weakly negatively charged silica particles in the early stages of the synthesis but, shortly after forming a stable multilayer, are unable to kinetically compete with silica self-aggregation (perhaps flocculation is more accurate) of small and growing secondarily nucleated silica particles. As a consequence, once the charge on gold is mostly screened by silica, shell growth stops (at about 4 nm under the conditions examined).

Secondary nucleation of silica particles was observed with both precursors. Any release of PVP into solution from the AuNP could seed secondary particles and exacerbate this situation. In the case of **2**, although silica formation was rapid, little secondary nucleation occurred at the early stages of the process. This facilitated the cleaning of the SiO_2−AuNP by centrifugation. Over time, with either precursor, the secondarily nucleated particles grew to sizes that made them difficult to separate from the SiO_2−AuNP using centrifugation.

When comparing the two silica precursors, **2** provides a potential advantage by operating at neutrality to rapidly form a silica shell of about 3−4 nm thickness on the surface of the AuNP. Secondary nucleation did not initially occur during the formation of these shells, which made it simple to isolate and wash the SiO_2−AuNP. Its deficits, however, include difficulty in forming silica shells of variable thickness under the conditions examined. As discussed below, the **2**-derived silica shells on gold are sufficiently thick that the difference in the absorbance maxima between nonaggregated and aggregated particles is less than that achieved with thinner TEOS-derived shells. Reduced silica shell thicknesses with the diglyceroxysilane precursor should be accessible with the use of lower diglyceroxysilane concentrations and addition of polyols to slow growth.[49] By contrast, growing silica shells with TEOS using the Stöber method uses more stringent conditions but allows one to reliably control shell thickness over a larger range. In addition, the precursor is more readily available.

Absorption Maxima as a Function of Shell Thickness. The presence of a layer of silica on unaggregated AuNP has previously been shown to shift the absorbance maximum from that of the original gold particle in a nonmonotonic, shell thickness dependent manner.[36] The range of shell thicknesses of the particles here was not large enough to display the previously reported

trend in absorbance. However, prior to aggregation, irrespective of the origin of the silica and similar to the previous report the particles exhibited absorbance maxima that were red-shifted by a few nm from that of the uncoated particle. The exception to this was Stöber growth shells that were grown for only 6.6 h, which exhibited a lambda max of 543 nm. It can be seen in Figure 2B that the silica shells are ill-formed and patchy. As a result, it seems likely that the incomplete shells did not colloidally stabilize the particles throughout the repetitive centrifugation cycles, but rather that the higher absorbance in this sole case actually reflects the presence of partly aggregated particles.

The main focus of the experiments described herein was the preparation of SiO_2−AuNP that would be convenient supports for biological entities[24] and still exhibit a large, easily detected shift in SPB upon aggregation. Therefore, our main interest was to understand the effect of silica shell thickness on the change in SPB during particle aggregation. An SPB shift allows use of the particles for colorimetric detection assays.

Changes in Absorption Maxima Upon SiO_2−AuNP Aggregation. The effect of interparticle distance on the extinction spectrum of two AuNP has examined by Zhong et al.[12] They calculated and plotted the wavelengths of maximal absorption of two 20 nm AuNP as a function of particle separation. The trend observed is remarkably similar to that shown in Figure 4. It displays a negative correlation that decreases in slope as the separation of the two particles increases. Rechberger et al. have also examined a two particle system experimentally and have found a trend with a similar profile.[14] Our experimental data complements these studies by extending to larger systems of particles in nonidealized conditions.

The change in maximum absorption wavelength with time can be explained in terms of aggregate size. The degree to which the absorption maximum is red-shifted is dependent on the aggregate size as has been illustrated by Zhong et al.[12] As the aggregates grow in size for a given shell thickness the absorbance maximum red shifts to a greater extent. Thus, aggregation of SiO_2−AuNP is not an instantaneous process and the observation of greater red shifts over time is evidence of increasing aggregate sizes (Figure 4A). Attempts to determine aggregate size by dynamic light scattering or various electron microscopic visualization techniques have, to date, been unsuccessful. Nevertheless, at a given time point aggregates can be assumed to be of similar size due to ionic "self stabilization". As the aggregates grow, repulsive interactions between aggregates increase so that a primary minimum aggregate size is reached.[7,8]

It should be noted that the architecture of the nanostructured materials influences the extent to which plasmons can interact with each other. Cong et al. have demonstrated in gold−silica−gold (core−shell−shell) nanorods that the plasmons of the shell and core interact strongly even at much thicker silica thicknesses than those described here.[51] Caution should therefore be utilized when extrapolating the properties from one nanoarchitecture to another as the spacial relationships between structures play a significant role.

A different study has examined the effect of coating gold nanoparticles with protein on the absorbance spectra of aggregates. When AuNP interparticle spacing was manipulated by a somewhat flexible coating, the protein lysozyme,[13] precipitates form rather than the aggregated colloidal dispersions described here. The UV absorbances of aggregated lysozyme/AuNP, with which different gold spacings were achieved using variable concentrations and variable orientation of the approximately

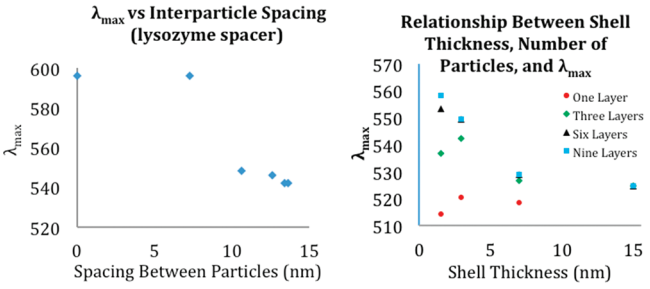

Figure 5. Correlation of red shift and interparticle spacing for: (A) 6.8 nm AuNP aggregated with a protein spacer at 23 °C, adapted from Verma et al.[13] (B) 13.2 nm core SiO_2−AuNP in multilayers, adapted from Ung et al.[11] note: all points overlap at 15 nm.

ovoidal protein, show an abrupt change between unmodified particles, and protein-coated gold in which the particle spacing is ∼10 nm (Figure 5A). Once the spacing reaches 10 nm, the protein layer is too thick to permit the gold particles to interact to a significant degree so that the absorbance maxima of the particles change little with increasing interparticle distances achieved by higher protein concentrations.

Multilayered films of SiO_2−AuNP have also been prepared using a layer-by-layer method.[11] The thickness of the silica shells ranged from 1.5 to 17.5 nm. This alternative approach directly produces analogues to the nanoparticle aggregates. The study found a negative correlation between shell thickness and maximum shift in SPB similar in profile to our data (Figure 5). For the thickest shells (>15.0 nm), there was no shift in SPB with increasing numbers of monolayers: the plasmons are not interacting. From a practical point of view, the shifts in the SPB once a shell thickness exceeds 4.6 nm become very small and, for the purposes of biological assays, impractical. There also was found a relationship between SPB shift and number of monolayers. This relationship runs parallel to our trend in increasing red shift with increasing aggregate size (longer aggregation times, Figure 4). In both cases, the extent of the red shift increases when more particles are able to interact with each other. All previous studies, both theoretical and experimental, show the utility of controlling the shell thickness (silica or protein) in order to manipulate interparticle distance upon aggregation. The maximum change in the wavelength of absorbance occurs when short (less than 5 nm) distances between the gold cores are utilized.

Liu has demonstrated the efficacy of silica-coated AuNP in biological assays by functionalizing SiO_2−AuNP with oligonucleotides and forcing aggregation via base pairing. The only disadvantage of the procedure is the necessity to follow aggregation processes via extinction coefficient. In this case, the thickness of the silica is large (35−90 nm), and there is very little change in the absorbance maximum, and therefore color, of the AuNP upon aggregation.[27−29]

In solution, as prepared here, SiO_2−AuNP undergo aggregation in the presence of salt. With thicker silica shells (>3 nm), the change in absorbance maxima upon aggregation is less pronounced (13−20 nm shift). Such particles, even if suitably modified with biological entities, will be less useful to monitor biological processes visually by the naked eye. By contrast, with thinner shells, < 3 nm, aggregation was accompanied by a larger increase in the absorbance maximum: the thinner the shell, the greater the shift (e.g., 527→558 nm shift − red to purple − in absorbance maximum upon aggregation with a shell thickness of

2.7 nm, Figure 1). With such silica shells, aggregation of the SiO_2−AuNP can be sensitively detected visually by the naked eye. Thus, such particles − suitably surface modified with biological entities − have the potential to be useful in biological assays when aggregation is controlled by biological events.

CONCLUSION

Thin shells of silica can be readily grown on AuNP using TEOS at high pH, or diglyceroxysilane **2** at neutral pH. Compound **2**-derived shells form rapidly and with reproducible thickness (∼3−4 nm) regardless of incubation time or concentration. By contrast, TEOS allows shell thickness to be tuned (1.7−4.3 nm using our method). The resulting SiO_2−AuNP undergo salt-induced aggregation leading to a change in absorption maxima that is dependent on shell thickness. The thinner silica shells (<3 nm) should be particularly useful for biological assays as the surface is amenable to tether biological molecules and the changes in color upon particle aggregation are readily discernible by eye.

ASSOCIATED CONTENT

Supporting Information. TEM images of original AuNP and SiO_2−AuNP, detailed data on shell thicknesses and absorption spectra, and plots of absorption spectra data from TEOS and **2** derived SiO_2−AuNP. This material is available free of charge via the Internet at http://pubs.acs.org/.

AUTHOR INFORMATION

Corresponding Author

*Fax: +1 905 522 2509. Tel: +1 905 525 9140 ext 23483. E-mail: mabrook@mcmaster.ca.

ACKNOWLEDGMENT

We thank Sentinel: NSERC Network on Bioactive Paper for financial support. We also thank Dr. Hanjiang Dong for helpful discussions, Professor Carlos Filipe for use of his centrifuge, and the staff at the McMaster University Faculty of Health Science Electron Microscopy Facility for their assistance.

REFERENCES

(1) Zhao, W.; Brook, M. A.; Li, Y. F. *ChemBioChem* **2008**, *9*, 2363–2371.
(2) Link, S.; El-Sayed, M. A. *J. Phys. Chem. B* **1999**, *103*, 4212–4217.
(3) Hill, H. D.; Mirkin, C. A. *Nat. Protocols* **2006**, *1*, 324–337.
(4) Daniel, M.-C.; Astruc, D. *Chem. Rev.* **2004**, *104*, 293–346.
(5) Zhao, W.; Lam, J. C. F.; Chiuman, W.; Brook, M. A.; Li, Y. *Small* **2008**, *4*, 810–816.
(6) Ghosh, S. K.; Pal, T. *Chem. Rev.* **2007**, *107*, 4797–4862.
(7) Mulvaney, P.; Liz-Marzán, L. M.; Geirsig, M.; Ung, T. *J. Mater. Chem.* **2000**, *10*, 1259–1270.
(8) Miller, K. T.; Zukoski, C. F. In *Semiconductor Nanoparticles—Physical, Chemical and Catalytic Aspects*; Meisel, D., Kamat, P., Eds.; Elsevier: Amsterdam, 1997; p 23−57.
(9) Mie, G. *Annal. Phys.* **1908**, *25*, 377–445.
(10) Brandl, D. W.; Mirin, N. M.; Nordlander, P. *J. Phys. Chem. B* **2006**, *110*, 12302–12310.
(11) Ung, T.; Liz-Marzán, L. M.; Mulvaney, P. J. *Phys. Chem. B* **2001**, *105*, 3441–3452.
(12) Zhong, Z.; Patskovskyy, S.; Bouvrette, P.; Luong, J. H. T.; Gedanken, A. *J. Phys. Chem. B* **2004**, *108*, 4046–4042.
(13) Verma, A.; Srivastava, S.; Rotello, V. M. *Chem. Mater.* **2005**, *17*, 6317–6322.
(14) Rechberger, W.; Hohenau, A.; Leitner, A.; Krenn, J. R.; Lamprecht, B.; Aussenegg, F. R. *Opt. Commun.* **2003**, *220*, 137–141.
(15) Su, K.-H.; Wie, Q.-H.; Zhang, X. *Nano Lett.* **2003**, *3*, 1087–1090.
(16) Harris, N.; Arnold, M. D.; Blaber, M. G.; Ford, M. J. *J. Phys. Chem. C* **2009**, *113*, 2784–2791.
(17) Marhaba, S.; Bachelier, G.; Bonnet, C.; Broyer, M.; Cottancin, E.; Grillet, N.; Lermé, J.; Vialle, J.-L.; Pellarin, M. *J. Phys. Chem. C* **2009**, *113*, 4349–4356.
(18) Portalès, H.; Pinna, N.; Pileni, M.-P. *J. Phys. Chem. A* **2009**, *113*, 4049–4099.
(19) Wang, M.-H.; Hu, J.-W.; Li, Y.-J.; Yeung, E. S. *Nanotechnology* **2010**, *21*, 145608.
(20) Huang, F.; Baumberg, J. J. *Nano Lett.* **2010**, *10*, 1787–1792.
(21) Halas, N. J. *ACS Nano* **2008**, *2*, 179–183.
(22) Plueddemann, E. P. *Silane Coupling Agents*, 2nd ed.; Plenum Press: New York, 1991.
(23) Liu, S.; Han, M.-Y. *Chem. Asian. J.* **2010**, *5*, 36–45.
(24) Hermanson, G. T. *Bioconjugate Techniques*, 2nd ed; Academic Press: New York, 2008.
(25) Campàs, M.; Katakis, I. *Anal. Chim. Acta* **2006**, *556*, 306–312.
(26) Masson, J.-F.; Battaglia, R. M.; Davidson, M. J.; Kim, Y.-C.; Prakash, A. M. C.; Beaudoin, S.; Booksh, K. S. *Talanta* **2005**, *67*, 918–925.
(27) Liu, S.; Zhang, Z.; Han, M. *Anal. Chem.* **2005**, *77*, 2595–2600.
(28) Liu, S.; Han, M. *Adv. Funct. Mater.* **2005**, *15*, 961–967.
(29) Liu, S.; Zhang, Z.; Wang, Y.; Wang, F.; Han, M.-Y. *Talanta* **2005**, *67*, 456–461.
(30) Graf, C.; Vossen, D. L. J.; Imhof, A.; Van Blaaderen, A. *Langmuir* **2003**, *19*, 6693–6700.
(31) Stöber, W.; Fink, A. *J. Colloid Interface Sci.* **1968**, *26*, 62–69.
(32) Mine, E.; Yamada, A.; Kobayashi, Y.; Konno, M.; Liz-Marzán, L. M. *J. Colloid Interface Sci.* **2003**, *264*, 385–390.
(33) Maye, M. M.; Han, L.; Kariuki, N. N.; Ly, N. K.; Chan, W.-B.; Luo, J.; Zhong, C.-J. *Anal. Chim. Acta* **2003**, *496*, 17–27.
(34) Woehrle, G. H.; Hutchison, J.; Özkar, E. S.; Finke, R. G. *Turkish J. Chem.* **2006**, *30*, 1–13.
(35) Brook, M. A.; Chen, Y.; Guo, K.; Zhang, Z.; Brennan, J. D. *J. Mater. Chem.* **2004**, *14*, 1469–1479.
(36) Liz-Marzán, L. M.; Geirsig, M.; Mulvaney, P. *Langmuir* **1996**, *12*, 4329–4335.
(37) Liz-Marzán, L. M.; Geirsig, M.; Mulvaney, P. *Chem. Commun.* **1996**, 731–731.
(38) Hall, S. R.; Davis, S. A.; Mann, S. *Langmuir* **2000**, *16*, 1454–1456.
(39) Zhu, H.; Pan, Z.; Hagaman, E. W.; Liang, C.; Overbury, S. H.; Dai, S. *J. Colloid Interface Sci.* **2005**, *287*, 360–365.
(40) Buining, P. A.; Humbel, B. M.; Philipse, A. P.; Verkleij, A. J. *Langmuir* **1997**, *13*, 3921–3926.
(41) Chen, M. M. Y.; Katz, A. *Langmuir* **2002**, *18*, 8566–8572.
(42) Lee, H. B.; Yoo, Y. M.; Han, Y.-H. *Scr. Mater.* **2006**, *55*, 1127–1129.
(43) Kanehara, M.; Watanabe, Y.; Teranishi, T. *J. Nanosci. Nanotechnol.* **2009**, *9*, 673–675.
(44) Han, Y.; Jiang, J.; Lee, S. S.; Ying, J. Y. *Langmuir* **2008**, *24*, 5842–5848.
(45) Robinson, S.; Williams, P. A. *Langmuir* **2002**, *18*, 8743–8748.
(46) Donatti, D. A.; Ruiz, A. I.; Vollet, D. R. *Ultrasonics Sonochem.* **2002**, *9*, 133–138.
(47) Donatti, D. A.; Vollet, D. R.; Ruiz, A. I. *J. Sol−Gel Sci. Technol.* **2000**, *18*, 5–9.
(48) Iler, R. K. *The Chemistry of Silica: Solubility, Polymerization, Colloid and Surface Properties and Biochemistry*; John Wiley & Sons; New York, 1979.
(49) Brook, M. A.; Chen, Y.; Guo, K.; Zhang, Z.; Jin, W.; Deisingh, A.; Cruz-Aguado, J.; Brennan, J. D. *J. Sol−Gel Sci. Technol.* **2004**, *31*, 343–348.
(50) Esumi, K.; Oyama, M. *Langmuir* **1993**, *9*, 2020–2023.
(51) Cong, H.; Toftegaard, R.; Arnjerg, J.; Ogilby, P. R. *Langmuir* **2010**, *26*, 4188–4195.